

Optical properties of high quality $\text{Cu}_2\text{ZnSnSe}_4$ thin films

F. Luckert,^{1,a)} D. I. Hamilton,¹ M. V. Yakushev,¹ N. S. Beattie,² G. Zoppi,² M. Moynihan,² I. Forbes,² A. V. Karotki,³ A. V. Mudryi,^{1,3} M. Grossberg,⁴ J. Krustok,⁴ and R. W. Martin¹

¹Department of Physics, SUPA, Strathclyde University, G4 0NG Glasgow, United Kingdom

²Northumbria Photovoltaics Applications Centre, Northumbria University, Ellison Building, Newcastle upon Tyne NE1 8ST, United Kingdom

³Scientific-Practical Material Research Centre of the National Academy of Science of Belarus, P. Brovki 19, 220072 Minsk, Belarus

⁴Tallinn University Technology, Ehitajate tee 5, Tallinn 19086, Estonia

(Received 1 April 2011; accepted 19 July 2011; published online 9 August 2011)

$\text{Cu}_2\text{ZnSnSe}_4$ thin films, fabricated on bare or molybdenum coated glass substrates by magnetron sputtering and selenisation, were studied by a range of techniques. Photoluminescence spectra reveal an excitonic peak and two phonon replicas of a donor-acceptor pair (DAP) recombination. Its acceptor and donor ionisation energies are 27 and 7 meV, respectively. This demonstrates that high-quality $\text{Cu}_2\text{ZnSnSe}_4$ thin films can be fabricated. An experimental value for the longitudinal optical phonon energy of 28 meV was estimated. The band gap energy of 1.01 eV at room temperature was determined using optical absorption spectra. © 2011 American Institute of Physics. [doi:10.1063/1.3624827]

The increasing cost and limited availability of indium, one of the main components in CuInSe_2 -based thin film solar cells, have resulted in a growing interest in the related semiconductor compounds $\text{Cu}_2\text{ZnSn}(\text{S},\text{Se})_4$, whose crystalline structure is similar to chalcopyrite with In substituted by alternating zinc (Zn) and tin (Sn). The possibility of *p*-type doping by intrinsic defects and a high absorption coefficient, exceeding 10^4 cm^{-1} , in the visible range¹ makes this new compound attractive for the application as an absorber layer in thin film solar cells. The recently reported conversion efficiency record of 9.6% (Ref. 2) demonstrates a high potential and makes this compound, containing neither expensive nor hazardous atomic species, a competitor to the chalcopyrite $\text{Cu}(\text{In},\text{Ga})\text{Se}_2$ as an absorber layer material for the large-scale production of thin-film solar cells.

Reliable knowledge of the essential fundamental electronic properties can significantly accelerate the development process of photovoltaic (PV) electronic devices. The most efficient technique for gaining such knowledge is optical spectroscopy [Refs. 3–5]. However, the usefulness of such methods depends critically on the availability of high quality material, with sharp and resolved features in the optical spectra. Despite the high record efficiency, the structural quality currently achieved in $\text{Cu}_2\text{ZnSn}(\text{S},\text{Se})_4$ is rather low; in the majority of publications, the photoluminescence (PL) spectra reveal only one broad, low intensity band ascribed to radiative recombination of free electrons and holes localised at shallow acceptors.⁶ The width of this band and its asymmetric shape suggest the influence of band tails induced by randomly distributed high concentrations of charged defects. Very little information on fundamental properties can be gained from the optical spectra of such material. Excitonic features in $\text{Cu}_2\text{ZnSnS}_4$ PL spectra have been reported by Hönes *et al.*⁷ However, no excitonic luminescence has so far been reported in $\text{Cu}_2\text{ZnSnSe}_4$ (CZTSe) due to the low quality

of the material. As a result, values for the energy of the CZTSe band gap, which is one of the most important material parameters for design of electronic devices, are found to vary from 0.8 in Ref. 8 to 1.62 eV in Ref. 9. Ahn *et al.* have discussed differences relating to phases, not detected by x-ray diffraction (XRD), and concluded that the CZTSe band gap is close to 1 eV.¹⁰

In this report, we demonstrate the possibility to fabricate excitonic grade CZTSe thin films, with PL spectra revealing an exciton peak as well as phonon replicas of a donor-acceptor pair (DAP) recombination providing an experimental value for the longitudinal optical (LO) phonon energy. The band gap energy is clarified using optical absorption (OA) spectra.

Thin films of CZTSe were fabricated by magnetron sputter deposition of Cu, Zn, and Sn from high-purity (5N) elemental targets as layered precursors on unheated substrates of either Mo-coated or bare soda-lime glass as described previously.¹¹ These precursors were then selenised at temperatures of 530 °C for 15 min in a mixture of Ar and Se vapour.

The morphology and elemental composition of the films were studied by scanning electron microscopy (SEM) combined with wavelength dispersive x-ray (WDX) microanalysis. The structural properties of the films and the presence of secondary phases were studied by XRD as well as by Raman spectroscopy. PL at temperatures from 4.2 to 300 K using a closed cycle cryostat and the 514 nm line of a 100 mW Ar^+ laser for excitation were employed to analyse opto-electronic properties. Optical transmission and reflection measurements were performed at room temperature in the spectral range from 600–1800 nm to establish the band gap value.

The cross-section of a film deposited on bare glass, shown in Fig. 1(a), reveals a dense homogeneous film with an average thickness of 700 nm. A quantitative WDX elemental composition line-scan, shown in Fig. 1(b), demonstrates good lateral homogeneity of the films. The ratios of the elements are $[\text{Cu}]/[\text{Zn} + \text{Sn}] = 1.05 \pm 0.02$, $[\text{Se}]/[\text{Cu} + \text{Zn} + \text{Sn}] = 0.91 \pm 0.01$, and $[\text{Zn}]/[\text{Sn}] = 0.94 \pm 0.03$,

^{a)} Author to whom correspondence should be addressed. Electronic mail: franziska.luckert@strath.ac.uk.

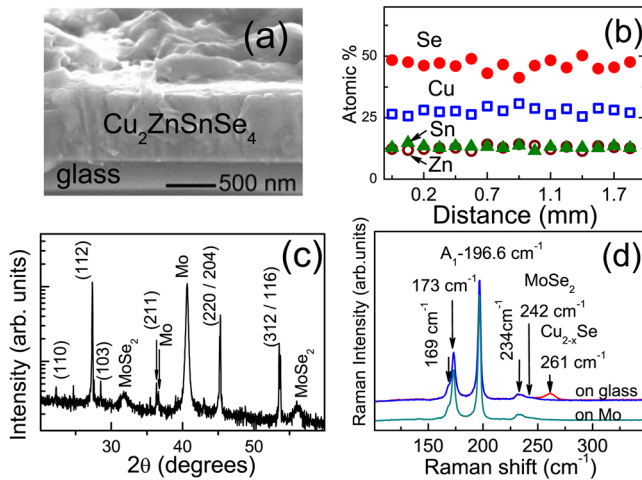


FIG. 1. (Color online) (a) Cross sectional SEM micrograph of a CZTSe film on glass, (b) WDX linescan, (c) XRD pattern of a CZTSe film on Mo, and (d) Raman spectra of the CZTSe thin films on glass and Mo.

indicating a small excess of copper as well as a deficiency of zinc and selenium.

Figure 1(c) shows the XRD spectrum of the CZTSe film on Mo on a logarithmic scale to highlight possible low intensity peaks. The spectrum reveals several distinct CZTSe peaks, a strong molybdenum peak, and two low intensity MoSe₂ peaks. These peaks imply that the selenisation reaction has continued through the precursor layer reaching the molybdenum substrate.

In the room temperature Raman spectra of the films on bare glass and Mo, shown in Fig. 1(d), the modes at 169, 173, 196.6, and 234 cm⁻¹, as reported earlier in Ref. 6 and assigned to CZTSe, can be seen. The Cu_{2-x}Se mode at 261 cm⁻¹, identified earlier,¹² can also be found at a few small spots randomly distributed across the surface. However, the main part of the surface was found to be free from secondary phases.

The 242 cm⁻¹ Raman line associated with MoSe₂ has rather low intensity when measured at the top of a dense, homogeneous film. Its intensity increases significantly (not shown here) when the laser beam is focused closer to the Mo layer suggesting that the MoSe₂ phase is present mainly at the Mo/CZTSe interface. The formation of the MoSe₂ phase has also been reported in Ref. 10 at the Mo/CZTSe interface after selenisation at 500 °C. None of the other secondary phases reported in Ref. 6 were observed in the Raman spectra of the CZTSe thin film.

The full width at half maximum (FWHM) of the dominant A₁ mode is 3 cm⁻¹. This is significantly smaller than the 10 cm⁻¹ estimated in the Raman spectrum, reported by Ahn *et al.*,¹⁰ and suggests superior structural quality for our material. In order to clarify the band gap energy, room temperature optical absorption $\alpha(h\nu)$ has been calculated using both optical transmission and reflection data.¹³ For an allowed direct transition, the spectral dependence of the absorption coefficient can be calculated as $\alpha = A(h\nu - E_g)^{1/2}/h\nu$ (Ref. 14) with constant A and optical band gap energy E_g . Fig. 3(a) plots a room temperature dependence of $(\alpha h\nu)^2$ on photon energy $h\nu$. The optical band gap of $E_g = 1.01$ eV has been determined by extrapolating the linear part of the

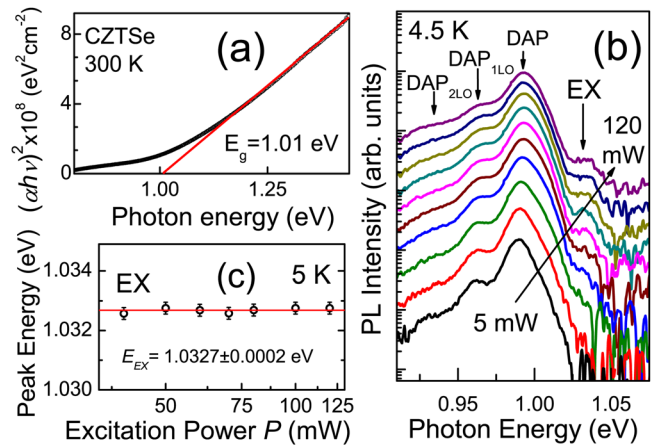


FIG. 2. (Color online) Room temperature dependence of $(\alpha h\nu)^2$ on photon energy $h\nu$ (a), evolution of the PL spectrum with increasing excitation power P (b), and excitation power dependence of the EX peak at 5 K (c).

$(\alpha h\nu)^2$ dependence to the photon energy axis. This value is in good agreement with those determined experimentally by Ahn *et al.* in Ref. 10 and Grossberg *et al.* in Ref. 6 as well as theoretically by Chen *et al.*¹⁵

Figure 2(b) shows the evolution of the near band edge PL spectra with changing excitation intensity. At 4.5 K, the PL spectra are dominated by a relatively narrow PL band at 0.989 eV (DAP) and the two lower intensity bands at 0.963 eV (DAP_{1LO}) and 0.932 eV (DAP_{2LO}). In order to determine their spectral positions and integrated intensity, the experimental data points of the DAP, DAP_{1LO}, and DAP_{2LO} have been fitted by three Gaussians. A small blue shift at a rate of 2.9 meV/decade, with increasing excitation power, suggests that the DAP peak originates from a donor-acceptor pair recombination.¹⁶

The integrated PL intensity of the DAP band increases with increasing excitation power P as $I \sim P^\gamma$, with the power coefficient $\gamma \approx 0.63$, suggesting that this band is due to defect related transitions.¹⁷ The spectral position of the DAP band maximum $h\nu_{max}$ can be described as

$$h\nu_{max} = E_g - (E_d + E_a) + \frac{e^2}{(4\pi\epsilon_0\epsilon r)}, \quad (1)$$

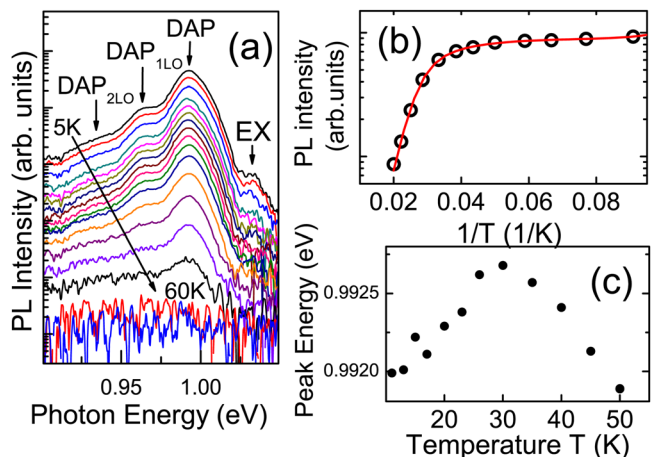


FIG. 3. (Color online) Temperature dependence of the PL spectra (a), temperature quenching of the integrated intensity of the DAP peak (○, experimental points; —, fitted lines) (b), and dependence of the DAP peak spectral position on temperature (c).

where E_d and E_a are the donor and acceptor ionisation energies, respectively, r is the distance between the donor and acceptor, e is the electron charge, ϵ is the static dielectric constant, and ϵ_0 is the permittivity of vacuum. The last term of Eq. (1) describes the Coulomb interaction between the donor and acceptor like defects. As the excitation power increases, the concentration of occupied donor and acceptor centres also increases, reducing the average distance between these defects resulting in a higher Coulomb interaction energy and a shift of the band towards higher energy.

The spectral positions of the two lower intensity bands DAP_{ILO} and DAP_{2LO} also shift towards higher energies with increasing excitation power at the same rate as the DAP band (2.9 meV/decade). The spectral distance between the DAP and the DAP_{ILO} bands as well as between the DAP_{ILO} and DAP_{2LO} bands is about ~ 28 meV, which is close to the LO phonon energy in the chalcopyrite CuInSe_2 .¹⁸ Therefore, DAP_{ILO} and DAP_{2LO} can be assigned to phonon-assisted DAP recombination with a LO phonon energy of $E_{\text{LO}} = 28 \pm 2$ meV ($226 \pm 16 \text{ cm}^{-1}$). The experimental uncertainty of determining the spectral position of the DAP bands in the PL spectra is such that the Raman line associated with LO phonons could be merged with the broad feature at 234 cm^{-1} .

The PL spectra, shown in Fig. 2(b), also reveal a high-energy feature (labelled EX) at ~ 1.033 eV. This feature can better be seen at higher excitation intensities and, as shown in Fig. 2(c), does not exhibit any shift with varying excitation power. The spectral position and the excitation power dependent behaviour of the EX feature suggest that this band can be attributed to a recombination of excitons. The evolution of the PL spectra with temperature increasing from 5 to 60 K is shown in Fig. 3(a). The intensity of all PL bands decreases. This temperature quenching is due to the thermally activated depopulation of the defect energy levels or/and to the activation of a non-radiative recombination centre. An Arrhenius plot can be used to determine activation energies E_a of the process. The exciton peak is quenching at around 13 K which makes it impossible to determine an activation energy value. The width and the quenching character of this feature suggest that it consists of non-resolved free and bound excitons.

Since the excitonic feature has been observed at liquid helium temperature, whereas the band gap measurements were carried out at room temperature, we cannot estimate the binding energy of the exciton. However, it is clear that the low temperature band gap energy should be quite close to the energy of the excitonic peak at 1.033 eV. The same low temperature band gap energy was recently confirmed by the temperature dependence of quantum efficiency spectra of CZTSe solar cells.¹⁹

The temperature quenching dependence of the integrated PL intensity for $T > 10$ K of the DAP band is shown in Fig. 3(b). The best fit of the experimental data points has been achieved assuming two activation energies,²⁰

$$I(T) = I_0 / \left[1 + A_1 \exp\left(-\frac{E_{a1}}{kT}\right) + A_2 \exp\left(-\frac{E_{a2}}{kT}\right) \right], \quad (2)$$

where I_0 (the intensity at the lowest temperature), E_a (activation energies), and A are fitting parameters (k is the Boltz-

mann constant). The determined activation energies are $E_{a1} = 27 \pm 3$ meV and $E_{a2} = 7 \pm 2$ meV. We propose a DAP model of recombination including an acceptor and a donor. With the temperatures increase, the DAP peak is becoming narrower and gradually shifting to higher energies due to the ionisation of the donor with an energy level 7 meV below the conduction band. The DAP recombination transforms into a recombination of an electron from the conduction band and a hole localised at the acceptor with an energy level 27 meV above the valence band.

In conclusion, CZTSe thin films have been studied by WDX, XRD, Raman, OA, and temperature resolved PL. The XRD and Raman spectra demonstrate high structural quality of the material. The band gap value, determined by optical absorption analysis at room temperature, was found to be close to 1 eV. The temperature quenching analysis of the dominating high-intensity and relatively narrow DAP band suggests that it is associated with the optical transitions between an acceptor at 27 meV above the valence band and a donor at 7 meV below the conduction band. Two phonon replicas of the DAP band and an excitonic feature have been observed in the PL spectra. An experimental LO phonon energy of ~ 28 meV was determined.

This work was supported by the EPSRC, Materials in Engineering (4.5.01) and SUPERGEN programme "Photovoltaics for the 21st Century," BCFR (F11MC-021), RFBR (10-03-96047 and 11-03-00063), and Estonian Science Foundation (G-8282).

¹K. Ito and T. Nakazawa, *Jpn. J. Appl. Phys.* **27**, 2094 (1988).

²T. K. Todorov, K. B. Reuter, and D. B. Mitzi, *Adv. Mater.* **22**, 1 (2010).

³M. V. Yakushev, A. V. Mudryi, I. V. Victorov, J. Krustok, and E. Melli-kov, *Appl. Phys. Lett.* **88**, 011922 (2006).

⁴M. V. Yakushev, F. Luckert, C. Faugeras, A. V. Karotki, A. V. Mudryi, and R. W. Martin, *Appl. Phys. Lett.* **97**, 152110 (2010).

⁵F. Luckert, M. V. Yakushev, C. Faugeras, A. V. Karotki, A. V. Mudryi, and R. W. Martin, *Appl. Phys. Lett.* **97**, 162101 (2010).

⁶M. Grossberg, J. Krustok, K. Timmo, and M. Altsaar, *Thin Solid Films* **517**, 2489 (2009).

⁷K. Hönes, E. Zscherpel, J. Scragg, and S. Siebentritt, *Physica B* **404**, 4949 (2009).

⁸T. M. Friedlmeier, N. Wieser, T. Walter, H. Dittrich, and H. W. Schock, *Proceedings of the 14th European Photovoltaic Specialists Conference, Barcelona* (H.S. Stephens & Ass., Bedford, UK, 1997), p. 1242.

⁹G. S. Babu, Y. B. K. Kumar, P. U. Bhaskar, and S. R. Vanjari, *Sol. Energy Mater. Sol. Cells* **94**, 221 (2010).

¹⁰S. Ahn, S. Jung, J. Gwak, A. Cho, K. Shin, K. Yoon, D. Park, H. Cheong, and J. H. Yun, *Appl. Phys. Lett.* **97**, 021905 (2010).

¹¹G. Zoppi, I. Forbes, R. W. Miles, P. J. Dale, J. J. Scragg, and L. M. Peter, *Prog. Photovoltaics* **17**, 315 (2009).

¹²G. Morell, R. S. Katiyar, S. Z. Weisz, T. Walter, H. W. Schock, and I. Bal-berg, *Appl. Phys. Lett.* **69**, 987 (1996).

¹³A. V. Mudryi, V. F. Gremenok, I. A. Victorov, V. B. Zalesski, F. V. Kurdesov, V. I. Kovalevski, M. V. Yakushev, and R. W. Martin, *Thin Solid Films* **431/432**, 193 (2003).

¹⁴J. I. Pankove, *Optical Processes in Semiconductors* (Dover, New York, 1975).

¹⁵S. Y. Chen, X. G. Gong, A. Walsh, and S. H. Wei, *Appl. Phys. Lett.* **94**, 041903 (2009).

¹⁶R. Dingle, *Phys. Rev.* **184**, 788 (1969).

¹⁷T. Schmidt, K. Lischka, and W. Zulehner, *Phys. Rev. B* **45**, 8989 (1992).

¹⁸H. Tanino, T. Maeda, H. Fujikake, H. Nakanishi, S. Endo, and T. Irie, *Phys. Rev. B* **45**, 13323 (1992).

¹⁹J. Krustok, R. Josepson, T. Raadik, and M. Danilson, *Physica B* **405**, 3186 (2010).

²⁰J. Krustok, H. Collan, and K. Hjelt, *J. Appl. Phys.* **81**, 1442 (1997).